Influence of shear strain on the hydrogen trapped in bcc-Fe: A first-principles-based study

Ryosuke Matsumoto[a, b, *], Yoshinori Inoue[c], Shinya Taketomi[a, b], Noriyuki Miyazaki[a, b]

[a] *Department of Mechanical Engineering and Science, Graduate School of Engineering, Kyoto University, Sakyo-ku, Kyoto 606-8501, Japan*

[b] *Visiting Researcher, National Institute of Advanced Industrial Science and Technology (AIST)*

[c] *Graduate Student, Department of Mechanical Engineering and Science, Graduate School of Engineering, Kyoto University*

Abstract

To advance our understanding of hydrogen related fractures of metals and alloys, it is essential to understand the influence of lattice defects and stress on the hydrogen existence state and its concentrations. In this study, we use density functional theory and interatomic potential to clearly show that shear strain in bcc-Fe yields strong hydrogen trap energy, comparable to that of volumetric strain.

Key words: hydrogen; iron; density functional; simulation; trap energy

Hydrogen is expected to find increasing use as an energy source in the near future, due to the escalation of environmental problems with current fuels. Although it is well known that hydrogen weakens the strength of most metals and alloys [1-4], the specific mechanisms remain a subject of debate. The construction of a secure hydrogen-energy-based society requires quantitative prediction of the strength of materials in a hydrogen environment.

Extensive research has reported that solute hydrogen atoms and lattice defects have strong interactions, and trapped hydrogen atoms significantly change the stability and/or mobility of defects [5-8]. Thus, knowing the hydrogen existence state and its concentrations around defects is critical. Sofronis et al. analyzed the hydrogen distribution around edge dislocations using a continuum model [9], and explained the promoted dislocation activity from the hydrogen shielding effect on the elastic interaction. Here, it is generally believed that hydrogen atoms accumulate at a high hydrostatic stress region, such as ahead of a mode I crack tip and under an edge-dislocation core. Many previous studies took into consideration the gradient of hydrostatic stress in the hydrogen diffusion equation [9-12]. However, it has long been known that interstitial atoms in bcc metals and alloys, such as the carbon atom in bcc-Fe, interact strongly with shear deformations [13]. Recent detailed analyses of the distributions of carbon around dislocations also revealed the importance of shear strain components [14]. Our atomistic study of the distribution of hydrogen trap energy around the edge dislocations in bcc-Fe showed that both hydrostatic and shear stress are necessary to explain the distribution [15].

The change in heat of solution caused by elastic strain is equivalent to the trap energy yielded by elastic strain for solute hydrogen atoms in a crystal lattice. In this paper,

first, we present the influence of elastic strain on the heat of solution of hydrogen incorporated in bcc-Fe using density functional theory (DFT), and compare the results with those from the embedded atom method (EAM) potential developed by Wen et al. (EAM (Wen) potential) [16]. After verifying the accuracy of the interatomic potential, we estimate the trap energy yielded by shear strain for various crystal orientations using the potential, for sufficiently large calculation models.

We performed DFT calculations within the spin-polarized generalized gradient approximation (GGA) [17] for electron exchange and correlation, using the Vienna Ab-initio Simulation Package (VASP) [18-20]. The interactions between the ions and electrons are described by Blöchl's projector augmented wave (PAW) method [21], which has an accuracy similar to an all-electron method within the frozen core approximation. The Monkhorst–Pack scheme [22] is used to define k-points, and the conjugate-gradient method is employed in the relaxation algorithm. We used $30 \times 30 \times 30$ k-points per unit lattice and 425 eV cut-off energy, which is sufficient for reliable calculations. Zero-point energy (ZPE) corrections, calculated from the Hessian matrix, were considered in all calculations. These calculation conditions provide good agreement with previous reports for typical physical properties of Fe-H systems [23, 24]. Using these calculation conditions, we obtained $E_0 = -16.416$ eV as the ground-state energy of a conventional bcc-Fe unit lattice containing two atoms, $L_0 = 0.2832$ nm as the relaxed lattice length of bcc-Fe, and $E_{H_2} = -6.524$ eV as the ZPE corrected ground-state energy of a hydrogen molecule. Here the ground-state energy is defined as the absolute total energy with respect to the origin of the total energy of free ions and electrons separated by an infinite distance.

There are two types of interstices in a bcc lattice: tetrahedral (t)-site and octahedral (o)-site. It is well known that, in bcc-Fe, hydrogen prefers to occupy a t-site rather than an o-site, whereas other interstitial atoms prefer to occupy an o-site rather than a t-site. However, it has been reported that o-site occupation becomes more stable under monoaxial tensile conditions for the hydrogen in bcc metals [25]; thus, o-site occupation possibly influences the hydrogen distribution around the stress singular points.

We introduced a hydrogen atom into a t- or an o-site in a strained bcc-Fe lattice consisting of $N = 16$ Fe atoms ($2 \times 2 \times 2$ lattices), and calculated the ground-state energy $E_{\mathrm{Fe}_N\mathrm{H}}\left(\varepsilon_{ij}, n\right)$. Here, n can be t- or o-site, and index i and j can be x, y, or z. According to conventional notation, we describe ε_{xx}, ε_{yy} and ε_{zz} as ε_x, ε_y and ε_z, respectively. We define the strain by Cauchy's infinitesimal strain tensor using the lattice size of bcc-Fe (L_o). Both occupation sites have an anisotropic geometry, as illustrated in Figs. 1(a) and (b); i.e., the occupation sites shown in Fig. 1(a) (t-site) and (b) (o-site) have the symmetrical property only in the y- and z-axes. We call them the t_x- and o_x-site, respectively. According to the symmetrical property of the occupation sites, here we apply two different tensile strains (ε_x and ε_y (= ε_z)) and two different shear strains (ε_{xy} and ε_{yz} (= ε_{zx})) for both t_x- and o_x-site occupations. The relationship for a different occupation site (t_y-, t_z-, o_y- or o_z-site) is easily obtained by changing indexes. The strain effects are estimated in the range of $\left|\varepsilon_{ij}\right| \le 0.05$, which is almost equal to the elastic strain around the dislocation core ($r > 0.5$ nm). All atomic positions are relaxed under fixed lattice conditions. The heat of solution for incorporation of hydrogen into the strained lattice, $E^{\mathrm{HOS}}\left(\varepsilon_{ij}, n\right)$, is estimated by

$$E^{\mathrm{HOS}}\left(\varepsilon_{ij},n\right)=E_{\mathrm{Fe}_N\mathrm{H}}\left(\varepsilon_{ij},n\right)-\left(N\times\frac{1}{2}E_0\left(\varepsilon_{ij}\right)+\frac{1}{2}E_{\mathrm{H}_2}\right), \quad (1)$$

where $E_0(\varepsilon_{ij})$ is the ground-state energy of the bcc-Fe unit lattice under strain ε_{ij}. $E^{\mathrm{HOS}}\left(\varepsilon_{ij},n\right)$ includes the influences of the nonlinear elasticity and the chemical interactions.

The heats of solution under tensile and shear strain are shown in Figs. 2(a) and (b), respectively. It is found that changes in the heats of solution notably differ according to the strain directions for the o-site occupation (Fig. 2(a)). This result corresponds to the large tetragonal strain caused by an o-site occupation. The heat of solution for incorporation of hydrogen into the o-site becomes almost the same as that into the t-site for $\varepsilon_x > 0.04$. The magnitudes of the changes of heat of solution from tensile strain (Fig. 2(a)) are much larger than those from shear strain (Fig. 2(b)) in this reference crystal, which is oriented in [100], [010] and [001] directions to the *x*-, *y*-, and *z*-axes, respectively. However, since the heat of solution for incorporation of hydrogen into the o-site is significantly influenced by the direction of tensile deformation, strong shear strain effects can appear for different crystal orientations, as shown later.

Although DFT calculations can give quantitative predictions for given atomic structures, the model size is small because of the calculation costs, and therefore, the results suffer from model size effects. Here we need to treat a deformed lattice, which has a low symmetrical property for a k-point configuration; thus, using a larger model is computationally too expensive. We consider using an interatomic potential that can overcome the size limitation.

Figure 2(c) shows the effect of tensile strain on the heat of solution estimated by the EAM (Wen) potential. We performed relaxation of the atomic positions and used the $N = 16$ ($2 \times 2 \times 2$ lattices) model, which is the same as that used for DFT calculations. Comparing Figs. 2(a) and (c) shows that, in spite of the high hydrogen concentration, the EAM (Wen) potential represents the changes in the heats of solution under elastic strain with good accuracy especially for the o-site occupations. It is also found in the EAM(Wen) potential calculations that hydrogen atoms occupy t-site under small deformations, as well as first principles calculations. The results under shear deformation are omitted because the range of the change is small, as for the DFT calculations. We consider that the difference in the heat of solution for incorporation of hydrogen into a t-site in an undeformed lattice between this calculation (0.33 eV) and the reference value (0.30 eV [26]) is mainly due to the elastic energy attributed to lattice dilatation.

We estimated the cell size influences by changing the number of lattices. The heat of solution for t-site occupation becomes almost constant for a unit cell size of $3 \times 3 \times 3$ lattice; however, for o-sites, we need a $4 \times 4 \times 4$ or even larger unit cell. We confirmed that a $10 \times 10 \times 10$ lattice model ($N = 2000$) is sufficiently large for both occupation sites. The strain effects on the heat of solution for the $10 \times 10 \times 10$ lattice model are shown in Fig. 2(d). The heats of solution for incorporation of hydrogen into the undeformed lattice are $E^{\mathrm{HOS}}(0, \mathrm{t\text{-}site}) = 0.29\,\mathrm{eV}$ and $E^{\mathrm{HOS}}(0, \mathrm{o\text{-}site}) = 0.32\,\mathrm{eV}$ for t- and o-site occupation, respectively, and these values are consistent with the previous large scale DFT calculations [23]. The potential can reproduce elastic constants accurately; therefore, we consider that the EAM (Wen) potential can predict the effect of strain on the heat of solution for various hydrogen concentrations, with at least $N \geq 16$ lattice models. Thus,

the relationship shown in Fig. 2(d) has (quantitatively) sufficient accuracy, without being affected by cell size limitations and high hydrogen concentration. It was found that t_x-site occupation becomes unstable for $\varepsilon_y > 0.01$ or $\varepsilon_y < -0.015$ ($\varepsilon_z > 0.01$ or $\varepsilon_z < -0.015$), and hydrogen moves toward a neighboring o_y-site (o_z-site); and thus we limited the curve for the small strain.

The contribution to the trap energy of strain ε_{ij} is expressed as

$$\Delta E^{\mathrm{trap}}\left(\varepsilon_{ij}, n\right) = -\left(E^{\mathrm{HOS}}\left(\varepsilon_{ij}, n\right) - E^{\mathrm{HOS}}\left(0, n\right)\right). \quad (2)$$

The strain effect on the hydrogen trap energy can be approximated using the amount of lattice dilatation caused by hydrogen. However, for hydrogen, the stable occupation site changes depending on the strain, and in some cases, different kinds of occupation sites combine into one or certain occupation sites disappear (Fig. 2 (d) and Ref. [15, 25]). Thus, the actual estimation of the relation is important.

We estimate the trap energy yielded by elastic strain $\boldsymbol{\varepsilon'}$ at the occupation site positioned at $\boldsymbol{x'}$ in a different crystal orientation as follows: (1) using the rotation tensor, the strain tensor $\boldsymbol{\varepsilon'}$ and the coordinates of the hydrogen occupation site $\boldsymbol{x'}$ are transformed to the reference coordinate system, where ΔE^{trap} was preliminarily estimated as a function of strain component ε_{ij} and occupation site n; (2) the occupation site is classified to t_x-, t_y- or t_z-site (or o_x-, o_y- or o_z-site); (3) the trap energy yielded by each strain component is obtained using $\Delta E^{\mathrm{trap}}\left(\varepsilon_{ij}, n\right)$; (4) the absolute contribution to trap energy from all strain components $\Delta E^{\mathrm{trap\_total}}$ is estimated as the linear sum of the trap energy yielded by each strain component; and, (5) finally, the trap energy E^{Trap} is estimated by considering the difference in the heat of solution between t- and o-sites at an undeformed

state (e.g., for o-site occupations in bcc-Fe; $E^{\mathrm{Trap}} = \Delta E^{\mathrm{Trap\_total}} + (H^{\mathrm{HOS}}(0, \text{t-site}) - H^{\mathrm{HOS}}(0, \text{o-site}))$.

Figure 3(b) shows the trap energy yielded by pure shear $\varepsilon_{x'y'}$ in the coordinate system, in which the [111], $[\bar{1}\,\bar{1}\,2]$ and $[1\,\bar{1}\,0]$ directions are defined as the x'-, y'- and z'-axes, respectively (Fig. 3(a)). Since t_x- and t_y-site occupations become unstable under the severe strain as mentioned in Fig.2 (d), the curve is limited for small stran in the figure. It is found that the trap energy is strongly dependent on the shear strain, and the sensitivity is nearly equal to that of the tensile strain in the reference crystal orientation (Fig. 2(d)). A small amount of shear strain ($\varepsilon_{x'y'} \approx 0.01$) changes the most stable occupation site from t_x-site (or t_y-site) to an o_z-site. Furthermore, although the energy difference among occupation sites is only 0.03 eV for an undeformed lattice, the difference becomes very large under strained condition (e.g., ~0.42 eV when $\varepsilon_{x'y'} = -0.05$ and ~0.1 eV when $\varepsilon_{x'y'} = -0.01$). Thus, the elastic strain makes the potential surface of hydrogen diffusion uneven, and the diffusion coefficient and diffusion pass are significantly altered by strain. We confirmed that the relationship obtained by the DFT calculations (Fig. 2(a) and (b)) also gives the similar curves.

The hydrogen trap energies yielded by a constant shear strain are calculated for various crystal orientations. The coordinate system shown in Fig. 4(a), where the $[1\,\bar{1}\,\bar{1}]$, [110] and $[1\,\bar{1}\,2]$ directions are defined as the x'-, y'- and z'-axes, respectively, is rotated around the y'-axis by θ (transformed from the $x'y'z'$ to the $x''y''z''$ coordinate system), and then rotated around the x''-axis by ϕ (transformed from the $x''y''z''$ to the $x'''y'''z'''$ coordinate system). Finally, the pure shear strain $\varepsilon_{x'''y'''} = 0.05$ is applied, and the

maximum value of hydrogen trap energy among the t_x-, t_y-, t_z-, o_x-, o_y-, and o_z-sites is estimated for various rotation angles. Figure 4(b) shows the dependence of the maximum trap energy from shear strain on the rotation angles θ and ϕ, and Fig. 4(c) shows the trap energy in the cross section of $\theta = 0$, which includes slip planes of edge dislocations in bcc-Fe, i.e. {110}, {112} and {123} planes. In the figures, the trap energy arising from volumetric strain $\varepsilon_v = 0.05$ is shown by blue lines (0.154 eV), and the maximum trap energies indicated by (■) and (□) in Fig. 3(b) are also shown. It is found that the maximum trap energy yielded from shear strain exceeds the value yielded by the same magnitude of volumetric strain in a wide range of crystal orientations. Therefore, for those crystal orientations, the hydrogen distributions around stress singular points are more influenced by shear strain than volumetric strain.

Although the shear strain effect can be stronger than volumetric strain, the value (maximum of ~0.2 eV in Fig. 4(b)) may not be sufficiently large to trap hydrogen at room temperature under a practical hydrogen concentration, because the hydrogen concentration in lattice sites is very low in bcc-Fe. However, remarkable influences appear when various strain contributions overlap. Moreover, the shear strain effects observed in this study should appear in bcc metals other than Fe, and even in other crystal structures, which have strong anisotropy of occupation sites, and the influence becomes significant for metals that absorb a large amount of hydrogen.

In this study, we first estimated the strain effects on the heat of solution for incorporation of hydrogen into bcc-Fe by DFT calculations, and compared the results with those from EAM (Wen) potential. After verifying the accuracy of the interatomic potential, we estimated the hydrogen trap energy yielded by shear strain for various

crystal orientations, using calculation models of sufficient size, and revealed the significant influence of shear strain. This result indicates that hydrogen distribution and diffusion behaviour are also influenced by shear strain.

Part of this research was supported by the “Fundamental Research Project on Advanced Hydrogen Science” funded by the New Energy and Industrial Technology Development Organization (NEDO).

References

[1] E.A. Steigerwald, F.W. Schaller, A.R. Troiano, Trans. Amer. Inst. Mining and Met. Eng. 218 (1960) 832.

[2] C.D. Beachem, Metal. Trans. 3 (1972) 437.

[3] G. Han, J. He, S. Fukuyama, K. Yokogawa, Acta Mater. 46 (1998) 4559.

[4] Y. Murakami, Int. J. Frac. 138 (2006) 167.

[5] P.J. Ferreira, I.M. Robertson, H.K. Birnbaum, Acta Mater. 47 (1999) 2991.

[6] Y. Tateyama, T. Ohno, Phys. Rev. B 67 (2003) 174105.

[7] G. Lu, Q. Zhang, N. Kioussis, E. Kaxiras, Phys. Rev. Let. 87-9 (2001) 095501.

[8] S. Taketomi, R. Matsumoto, N. Miyazaki, J. Mater. Sci. 43 (2008), 1166.

[9] P. Sofronis, H.K. Birnbaum, J. Mech. Phys. Solids 43 (1995) 49.

[10] A.H.M. Krom, A. Bakker, R.W.J. Koers, Int. J. Pressure Vessels Piping 72 (1997) 139.

[11] H. Kotake, R. Matsumoto, S. Taketomi, N. Miyazaki, Int. J. Pressure Vessels Piping 85 (2008) 540.

[12] Y. Liang, D.C. Ahn, P. Sofronis, R.H. Dodds Jr, D. Bammann, Mech. of Mater. 40 (2008) 115.

[13] A.W. Cochardt, G. Schoek, H. Wiedersich, Acta Metal. 3 (1955) 533.

[14] E. Clouet, S. Garruchet, H. Nguyen, M. Perez, C.S. Becquart, Acta Mater. 56 (2008) 3450.

[15] S. Taketomi, R. Matsumoto, N. Miyazaki, Acta Mater. (2008). (in press) (doi:10.1016/j.actamat.2008.04.011).

[16] M. Wen, X.J. Xu, S. Fukuyama, K. Yokogawa, J. Mater. Res. 16-12 (2001) 3496.

[17] J.P. Perdew, Y. Wang, Phys. Rev. B 45 (1992) 13244.

[18] G. Kresse, J. Hafner, Phys. Rev. B 48 (1993) 13115.

[19] G. Kresse, J. Furthmüller, Phys. Rev. B 54 (1996) 11169.

[20] G. Kresse, J. Furthmüller, Comput. Mater. Sci. 6 (1996) 15.

[21] P.E. Blöchl, Phys. Rev. B 50 (1994) 17953.

[22] H.J. Monkhorst, J.D. Pack, Phys. Rev. B 13 (1976) 5188.

[23] D.E. Jiang, E.A. Carter, Phys. Rev. B 70 (2004) 064102.

[24] D.C. Sorescu, Catalysis Today 105 (2005) 44.

[25] Y. Fukai, J Less-Common Met. 101 (1984)1.

[26] J.P. Hirth, Metall. Trans. A 11 (1980) 861.

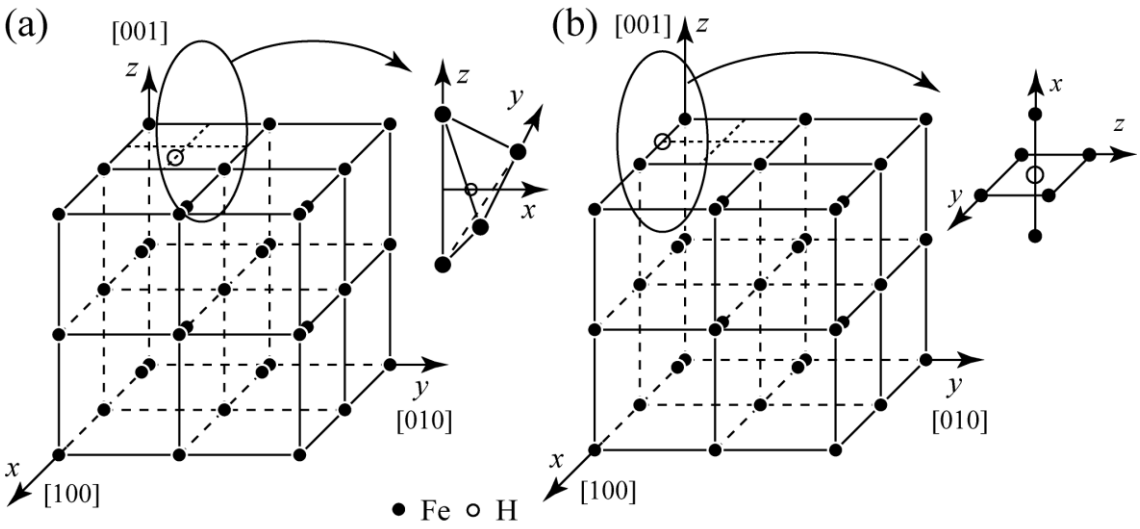

Figure 1. Bcc-Fe lattices consist of $N = 16$ Fe atoms ($2 \times 2 \times 2$ lattices) and one hydrogen atom: (a) and (b) show the t_x- and o_x-site occupations, respectively.

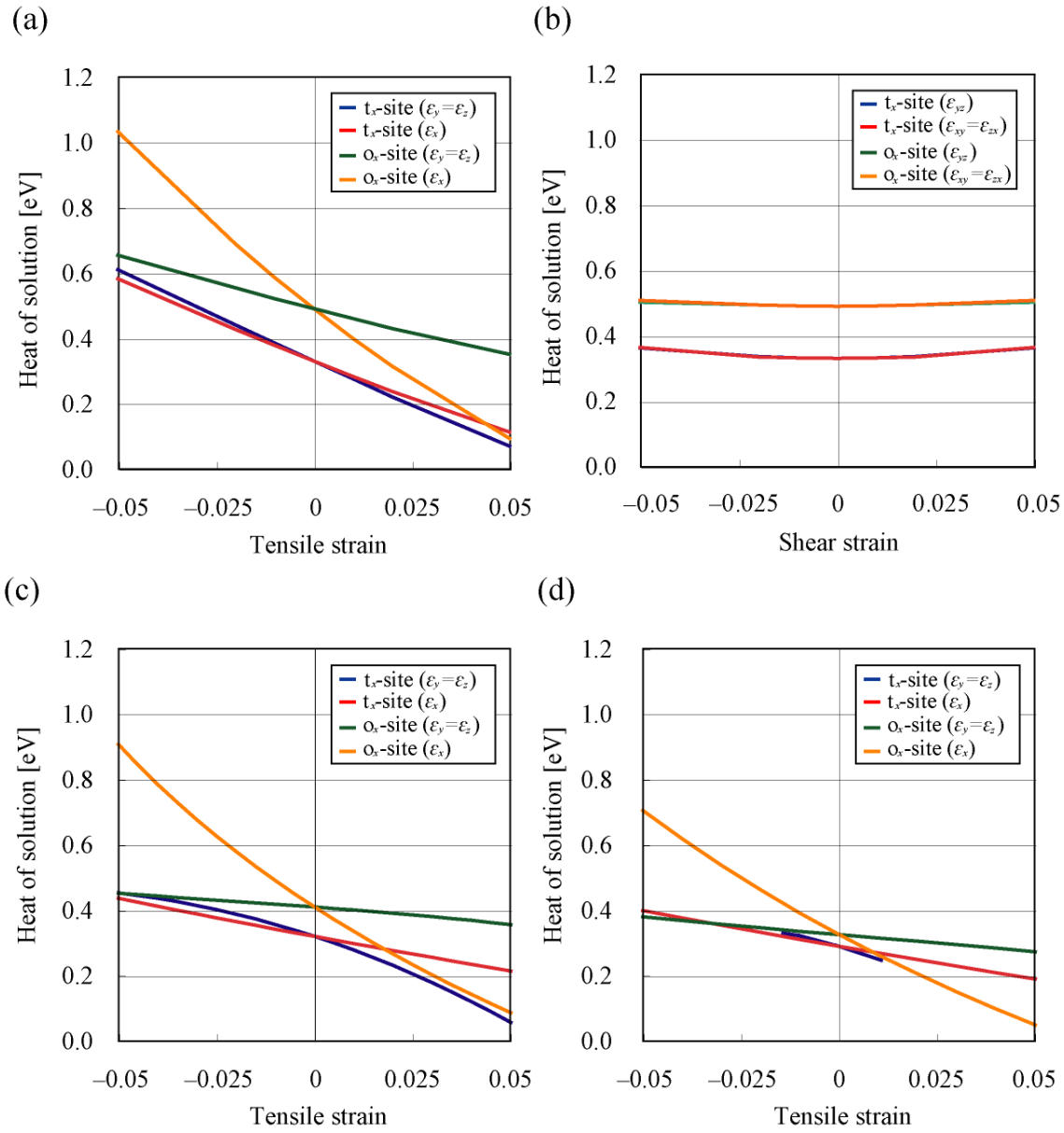

Figure 2. (colour online) Strain effects on the heat of solution of incorporation of hydrogen into bcc-Fe: (a) and (b) show the tensile and shear strain effects estimated by DFT calculations, respectively. (c) and (d) show the heats of solution into tensile strained bcc-Fe estimated by the EAM (Wen) potential for 2 × 2 × 2 and 10 × 10 × 10 lattices, respectively.

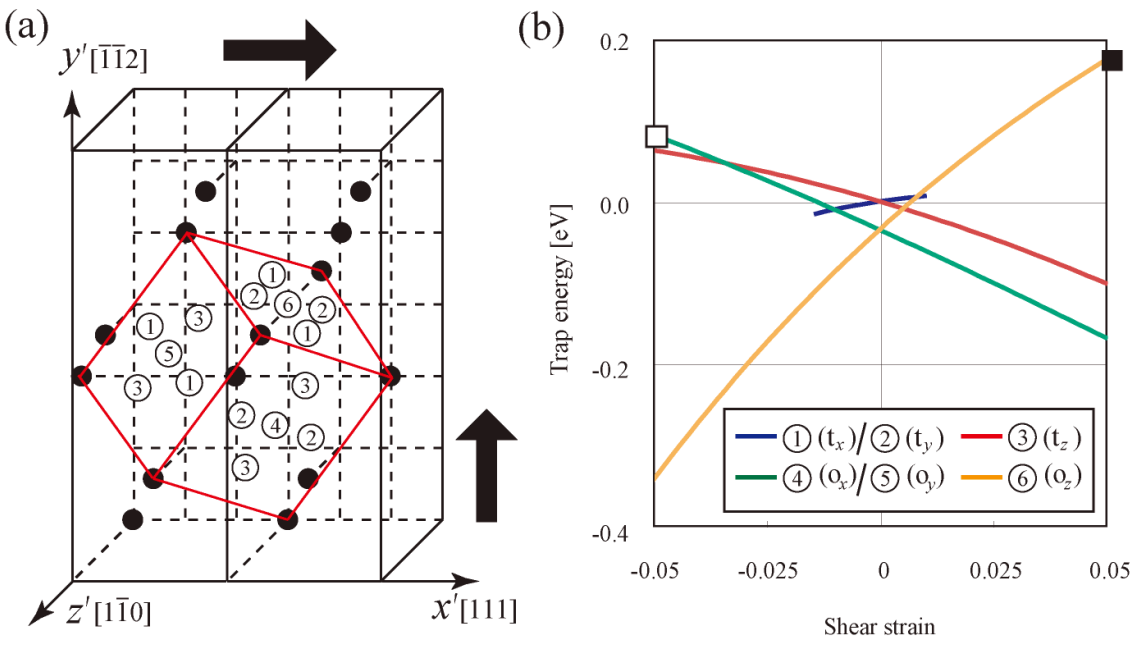

Figure 3. (colour online) Hydrogen trap energy yielded by pure shear $\varepsilon_{x'y'}$ in the coordinate system, where the [111], $[\bar{1}\,\bar{1}\,2]$ and $[1\,\bar{1}\,0]$ direction are defined as the x', y' and z'-axes, respectively. (a) The schematic diagram of the crystal structure and hydrogen occupation sites. (b) The relationship between shear strain and hydrogen trap energy. The symbol ■ is the maximum trap energy for $\varepsilon_{x'y'} = 0.05$, and □ is that for $\varepsilon_{x'y'} = -0.05$. These points correspond to those shown in Fig. 4(c).

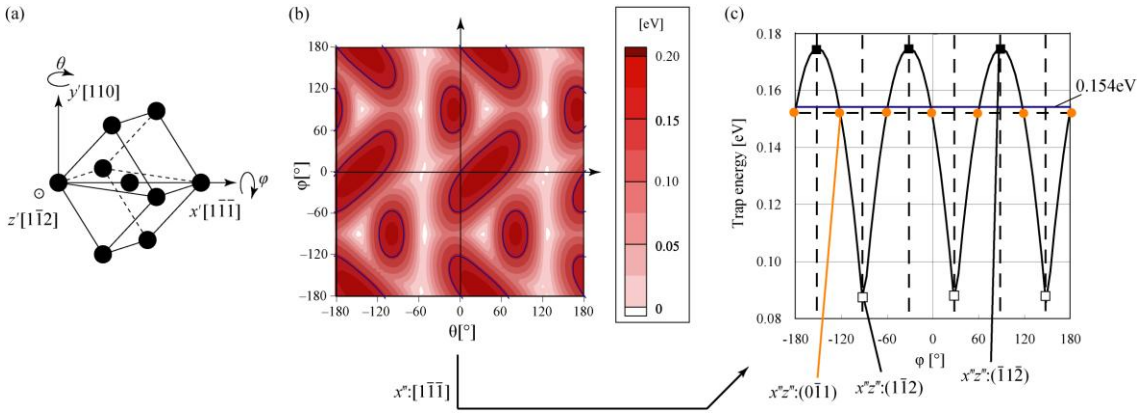

Figure 4. (colour online) Hydrogen trap energy yielded by shear strain for various crystal orientations. (a) The schematic diagram of crystal orientation. (b) The dependence of the maximum trap energy from shear strain on the rotation angles θ and ϕ. (c) The trap energy in the cross section of $\theta = 0$.